JOURNAL OF AIRCRAFT
Vol. 41, No. 4, July–August 2004

Small Disturbance Euler Simulations for Delta Wing Unsteady Flows due to Harmonic Oscillations

Caroline Weishäupl* and Boris Laschka†
Technische Universität München, 85747 Garching, Germany

Unsteady aerodynamic forces for aeroelastic analyses may be calculated by Euler or Navier–Stokes codes. Because of the large number of parameters, the computation times and costs become very high and the iteration process for a flutter free configuration could become quite lengthy. Therefore, classical potential methods are still widely used, and advanced codes are applied punctually in critical ranges for validation or refinement only. At the Institute for Fluid Mechanics (FLM) of the Technische Universität München it was proposed since 1998 to make use of the fact that the unsteady forces required for aeroelastic stability investigations are usually related to small displacements of the aircraft structure. They are, in general, only a small fraction of the occurring steady forces. Therefore, the Euler or Navier–Stokes equations may be developed for small displacements in the frequency domain, realized for inviscid flow in the FLM small disturbance Euler code, FLM–SDEu. After a comprehensive validation, here FLM-SDEu is applied to a cropped delta wing with 53-deg leading-edge sweep, investigating rigid body, flap, and elastic harmonic motions. Compared to the full Euler solution, the accuracy of FLM–SDEu is very good, and the required computer time is reduced by an order of magnitude.

Nomenclature

c_L	=	lift coefficient
c_M	=	pitching moment coefficient (related to x_m)
c_p	=	pressure coefficient
c_r	=	root chord length
f	=	frequency, Hz
k	=	reduced frequency, $2\pi c_r\sqrt{(\rho_\infty)}f/[\sqrt{(p_\infty\gamma)}M]$
M	=	Mach number
p	=	pressure
s	=	half-span
t	=	time
x, y, z	=	Cartesian coordinates
x_m	=	axis of reference
x_p	=	pitching axis
α	=	angle of attack
γ	=	ratio of specific heats
δ	=	geometric variable
η	=	flap deflection angle
ρ	=	density
τ_s	=	characteristic time, $\sqrt{(p_\infty\gamma)}Mt/[\sqrt{(\rho_\infty)}c_r]$
ϕ	=	sweep angle

Subscripts

0	=	mean value
1	=	amplitude

Superscript

1	=	first harmonic

Introduction

FOR the aeroelastic analysis process, one of the main issues is the adequate performance of the occuring steady and unsteady aerodynamic loads. Adequate means an appropriate method with reference to accuracy and speed. Methods based on potential theory are fast, but they have limitations in predicting flows with shocks properly. Euler and Navier–Stokes methods yield high-quality results with a proper resolution of shocks, but the computational costs and times are high especially for unsteady cases. To make use of the higher nonlinear modeling of flow physics by computational fluid dynamics (CFD) at acceptable numerical cost, numerous efforts are done in the field of reduced-order models, like Volterra series for identification of nonlinear systems in the time domain[1] or proper orthogonal decomposition to reduce the size of the involved matrices.[2]

The small disturbance Euler (SDEu) method FLM–SDEu developed at the Institute for Fluid Mechanics (FLM) of the Technische Universität München (TUM),[3,4] following some previous work in turbomachinery,[5–8] contributes to making high-quality CFD results usable. The basis for the small disturbance method was the nonlinear Euler code FLM–Eu of FLM–TUM.[4,9] This code is a shock-capturing method based on a finite volume approach with Roe's flux difference splitting.[10] Second-order accuracy in space is achieved due to MUSCL extrapolation for the conservative variables and the total–variation–diminishing property is guaranteed. Explicit and implicit time integration is available. For implicit time integration the lower-upper-symmetric successive overrelaxation (LU–SSOR) scheme, which was initially introduced by Jameson and Turkel[11] is applied. The small disturbance method FLM–SDEu is formulated consistently to the nonlinear method, described in detail in Refs. 3, 4, and 12. There it is assumed that the unsteady flow part is small compared to the steady mean flow. The unsteady problem can be reduced to a steady-state problem for the perturbation part. In this way, the unsteady loads can be evaluated directly. A reduction of an order of magnitude of computational time is achieved, by retaining the required accuracy. If we assume a harmonic motion for the unsteady perturbation part, the method is compatible with modal aeroelastic analysis. FLM–SDEu was validated for two-dimensional cases in subsonic, transonic, and supersonic flow. In three dimensions, the transonic flow around the high aspect ratio LANN wing was studied, and FLM–SDEu was compared to the results of several Euler codes with very good results.[3,4,13]

From this experience with FLM–SDEu, the next step is to apply this method to more complex geometries. Here a low aspect ratio cropped delta wing is investigated as a frequent high maneuverable aircraft case characterized by leading-edge vortices at higher angle of attack. For a transonic Mach number $M = 0.8$, harmonic motions on moderate angles of attack are investigated using FLM–SDEu. First, pitching oscillations for several angles of attack are

Presented as Paper 2000-0124 at the 38th Aerospace Sciences Meeting and Exhibit, Reno, NV, 10 January 2000; received 8 September 2002; revision received 23 September 2003; accepted for publication 29 September 2003.

*Chief Scientist, Institute for Fluid Mechanics. Senior Member AIAA.
†Chair, Institute for Fluid Mechanics. Honorary Fellow AIAA.

considered to show the applicability of the code. Then, as one of the essential features for the maneuverability of high maneuverable aircraft, inboard and outboard oscillating flaps efficiencies have been investigated.[12,14] Finally, elastic motions of the delta wing defined by polynomials are procured, which may be used to calculate generalized air forces for flutter analysis.[15,16] For validation, the results obtained from FLM–SDEu are compared with those of the corresponding nonlinear code FLM–Eu.

The theory and numerical features of FLM–SDEu and the solution procedure are described in detail in Refs. 3, 4, and 12. Therefore, in this paper emphasis is laid on the application of FLM–SDEu to a delta wing. The main characteristics concerning grid generation and the used grids are described, and results for the different harmonic motions are presented and discussed in detail. Lift and pitching moment coefficients as well as local pressure distributions are analyzed.

Geometry and Grid Generation

The investigations are performed for a delta wing with 53-deg leading-edge sweep and −3-deg trailing-edge sweep. The nondimensionalized root chord is $c_r/s = 1.6$, and the maximum relative thickness is $d/c_r = 4.7\%$. The wing has a round leading edge and is equipped with an inboard and an outboard flap (Fig. 1).[12,14]

For discretization, a CH topology is used for all considered cases. For all grids, the far-field distance is selected to 10 root chords for x and z directions and 5 root chords in the spanwise direction. The start grids are generated with the grid-generation tool MegaCads of the DLR, German Aerospace Research Center.[17] The smoothing is done with the inhouse tool GRIDFLM, based on a Poisson algorithm. The iterative process leads to a smooth grid with respect to orthogonality and continuous cell growth. For the unsteady simulations performed with FLM–SDEu or FLM–Eu, a second grid for the extremum position or the maximum deformation is necessary. The far field remains unchanged.

For the pitching oscillations and the elastic modes, the flaps need not be considered in detail. The volume grid consists of $180 \times 66 \times 30$ cells, with 60 cells chordwise and 36 cells spanwise on each wing side, and an off-body distance of the first gridline of $0.005s$ (Fig. 2). The number of overall cells is 356,400. To study the influence of the grid resolution, a finer grid is generated for the reference position. It consists of $230 \times 81 \times 35 = 652{,}050$ cells.

For a simulation of flap oscillations, the spatial discretization of the physical domain is again accomplished with a CH topology with $180 \times 66 \times 30$ cells. There are 60 cells chordwise and 36 cells spanwise used for the lower and upper wing side, respectively. Each flap is discretized with 15 cells chordwise and 12 cells spanwise. In the region of the flap leading and side edges, the grid points are concentrated for optimal resolution of flow gradients (Fig. 3). The pitching oscillations of the flaps are performed around the flap leading edge. A narrow region is introduced between the rigid wing and the flaps to realize a smooth change in surface during flap deflections. The gaps at the flap edges are not modeled. As a consequence, the wing surface is discretized as a continuous surface, as shown in the surface grid for an inboard flap deflection of −5 deg and an outboard flap deflection of 5 deg (Fig. 3). The distance of the first off-body grid line is fixed to $0.008s$. Further details of the grid for the flap oscillations may be found in Refs. 12 and 14.

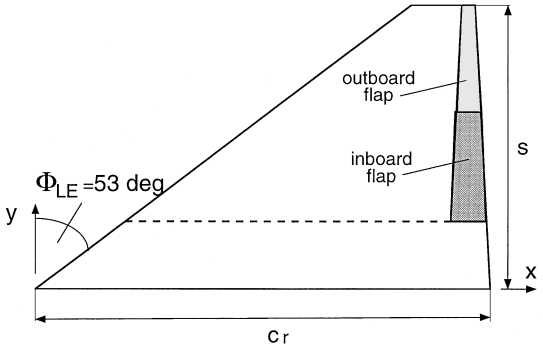

Fig. 1 Geometry and parameters of the delta wing.

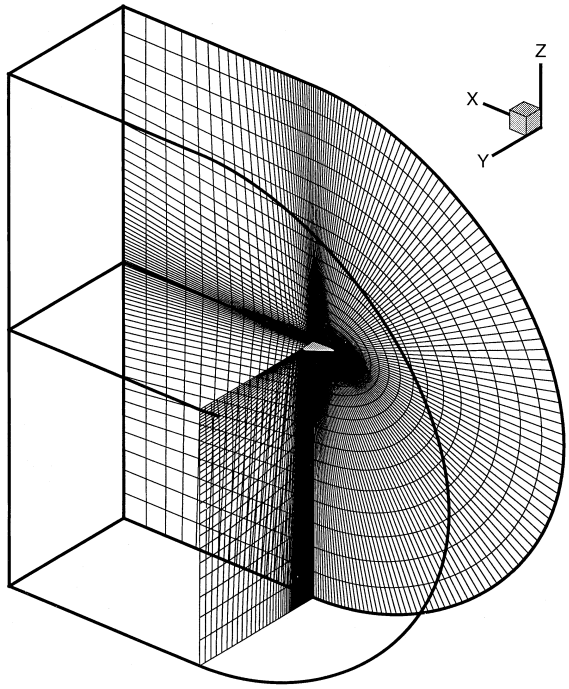

Fig. 2 Space grid for the delta wing in CH topology.

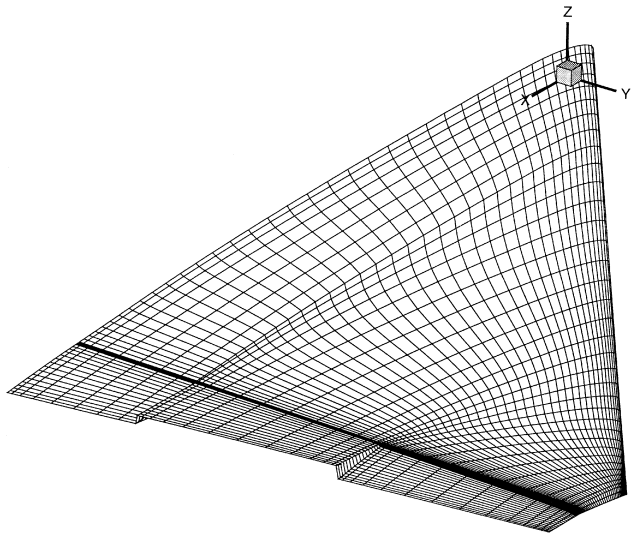

Fig. 3 Surface grid of the delta wing with flap deflection: $\eta_{\text{inboard}} = -5$ deg and $\eta_{\text{outboard}} = 5$ deg.

Results

Results are presented for several harmonic motions of the delta wing, describing the dependency of the regarded geometric variable δ by

$$\delta(\tau_s) = \delta_0 + \delta_1 \sin(k\tau_s) \tag{1}$$

with the mean value δ_0, the amplitude δ_1, the reduced frequency $k = 2\pi c_r \sqrt{(\rho_\infty)} f/[\sqrt{(p_\infty \gamma)} M]$, and the characteristic time $\tau_s = \sqrt{(p_\infty \gamma)} Mt/[\sqrt{(\rho_\infty)} c_r]$. The pitching moment reference axis is $x_m = 0$. All simulations are performed for the transonic Mach number $M = 0.8$, at which the angle of attack is varied between 0 and 15 deg. The steady state is assumed to be achieved if the absolute value of the overall density change related to the corresponding density change in the first time step is lower than 10^{-6}. The residual chosen for the solution of the SDEu equations and for the dual time stepping within LU–SSOR is 10^{-5}.

Steady Results

Steady simulations are presented for 0-, 5-, and 10-deg angle of attack. The dominant features are visualized in (Fig. 4) with Mach number contour plots and crossflow velocity vector plots in a grid plane close to the trailing edge for the three angles of attack. For these flowfields, the standard grid for the rigid-body motions has been taken. For $\alpha = 0$ and 5 deg, the flow is attached over the whole wing surface. Higher crossflow velocities are restricted to the tip region associated with the tip vortex. For 0-deg angle of attack, the flow turns from the upper to the lower side, corresponding to a negative lift coefficient. For $\alpha = 5$ and 10 deg, the lift coefficient is positive and the flow turns from the lower to the upper side. For $\alpha = 10$ deg, the level of crossflow velocity components is increased. In addition to the stronger tip vortex, a field of higher crossflow velocities, resulting from the leading edge, occurs. A weak leading-edge vortex develops. Given that the mechanism of forming a leading-edge vortex for a round leading edge is not physically driven in an Euler code, the correct representation of such a formation is less important for the main aim of the paper, namely, demonstrating the quality of the small disturbance method FLM–SDEu with respect to the nonlinear code.

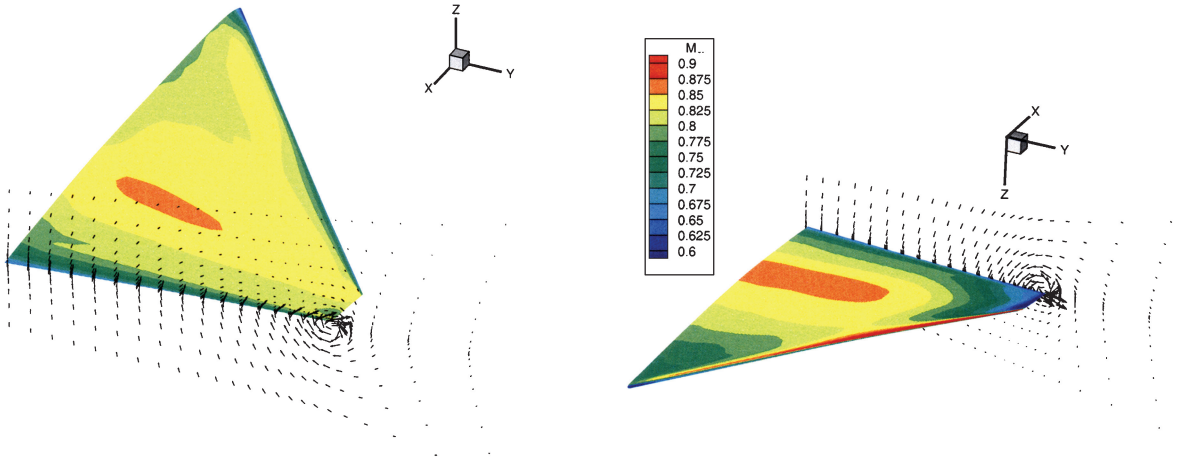

a) $\alpha = 0$ deg

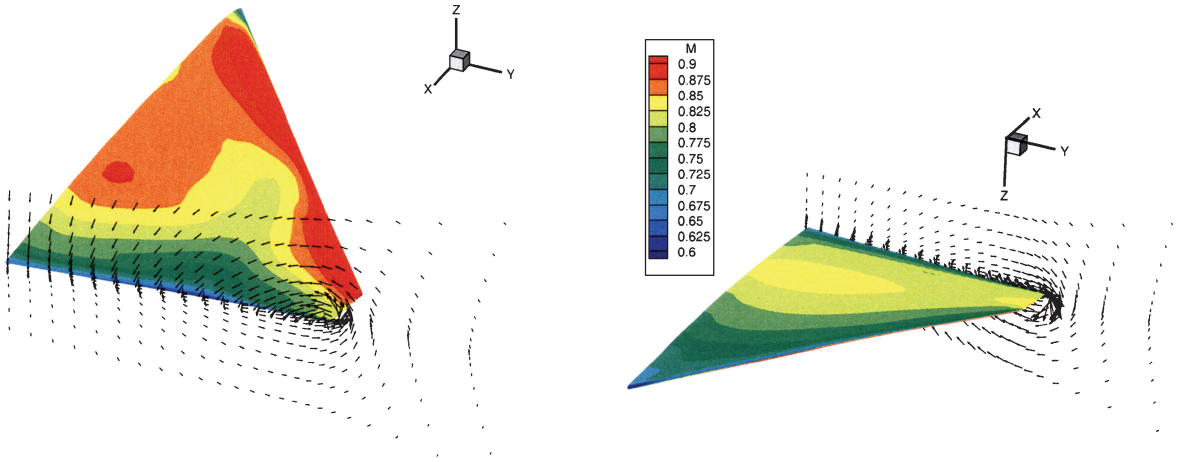

b) $\alpha = 5$ deg

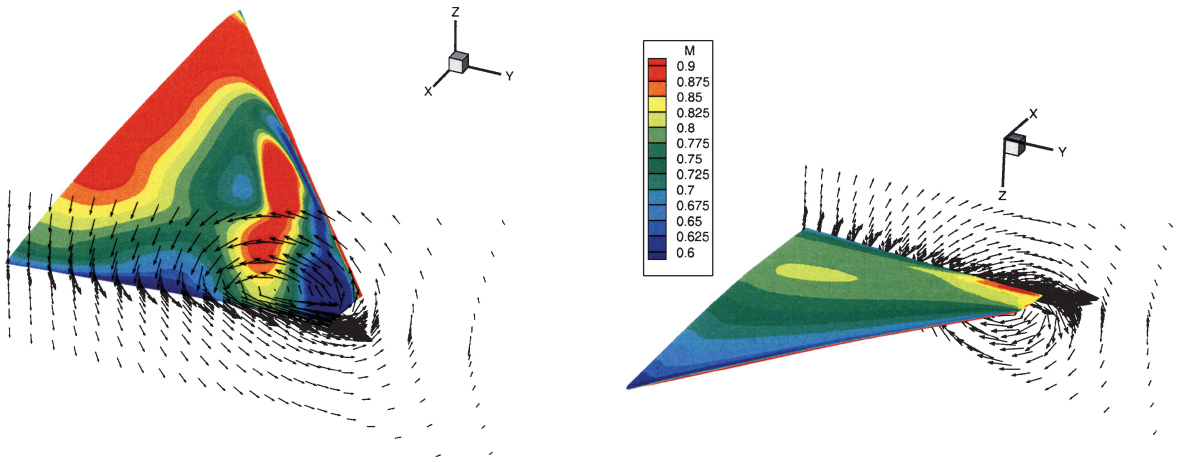

c) $\alpha = 10$ deg

Fig. 4 Steady flowfields with Mach number contour plot and crossflow velocity vectors at $M = 0.8$ and various α; upper side (left) and lower side (right).

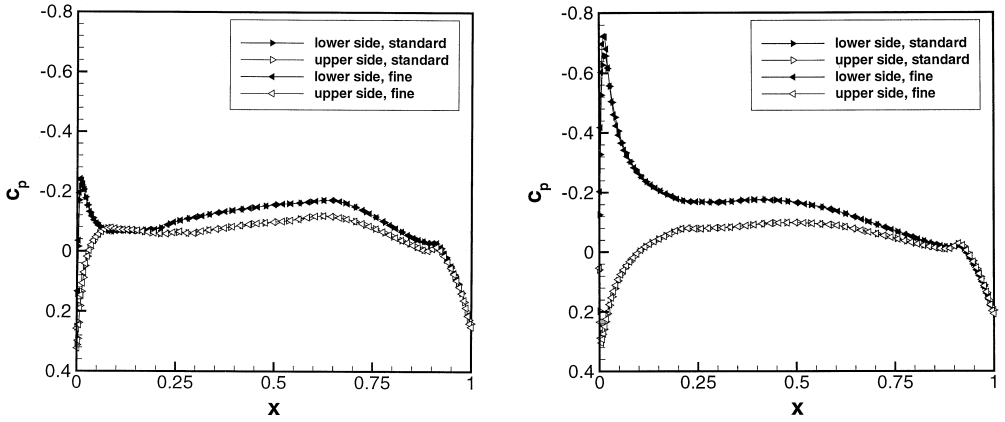

a) $y/s = 0.35$ b) $y/s = 0.75$

Fig. 5 Comparison of the steady pressure distribution c_p for standard and fine grid for $\alpha = 0$ deg at $M = 0.8$ in spanwise sections $y/s = 0.35$ and $y/s = 0.75$.

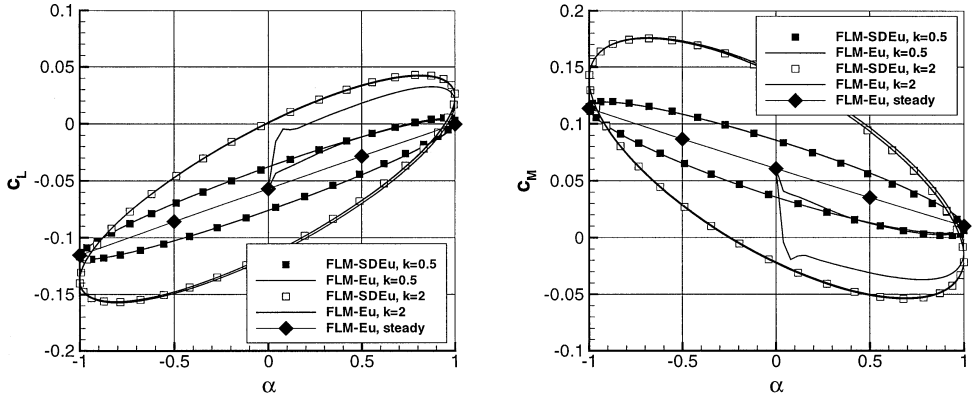

a) $\alpha = 0$ deg

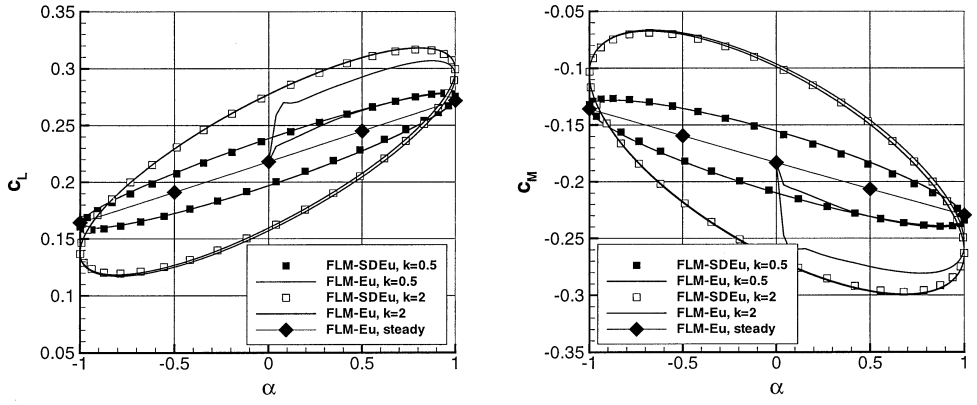

b) $\alpha = 5$ deg

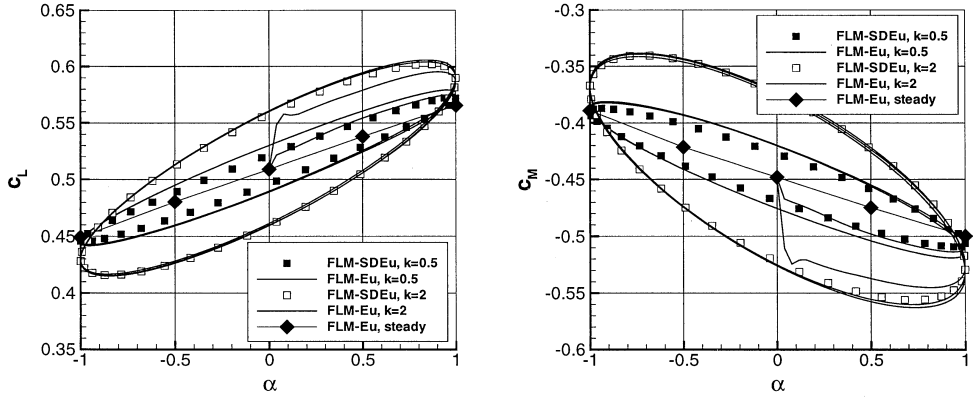

c) $\alpha = 10$ deg

Fig. 6 Lissajous figures of the lift and pitching moment coefficient for pitching oscillations for $M = 0.8$ at various α for $k = 0.5$ and 2.0.

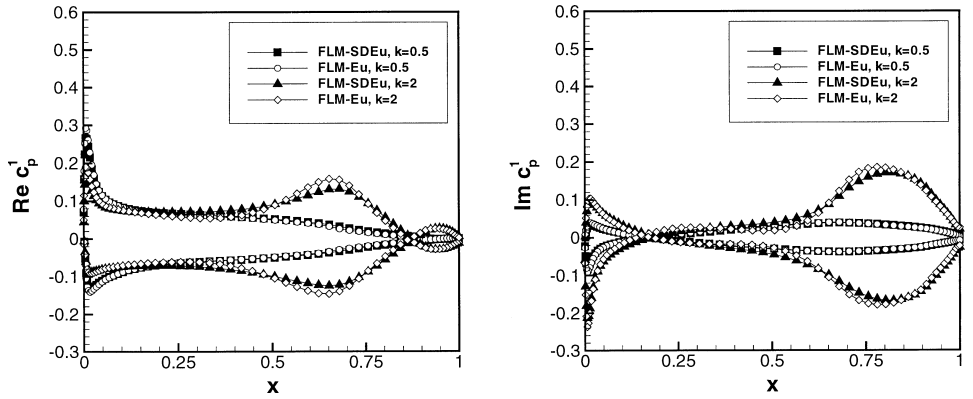

a) $y/s = 0.35$

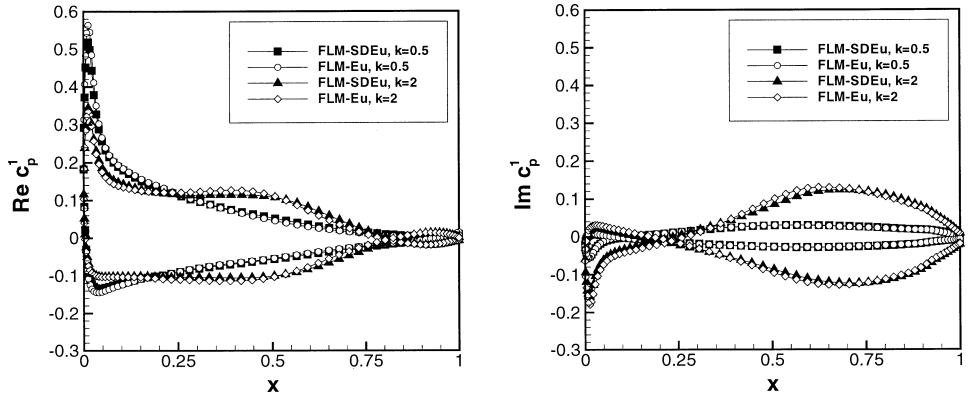

b) $y/s = 0.75$

Fig. 7 Real and imaginary part of the first harmonic of the pressure distribution for pitching oscillations for $\alpha = 0$ deg at $M = 0.8$ for $k = 0.5$ and 2.0 in spanwise sections $y/s = 0.35$ and $y/s = 0.75$.

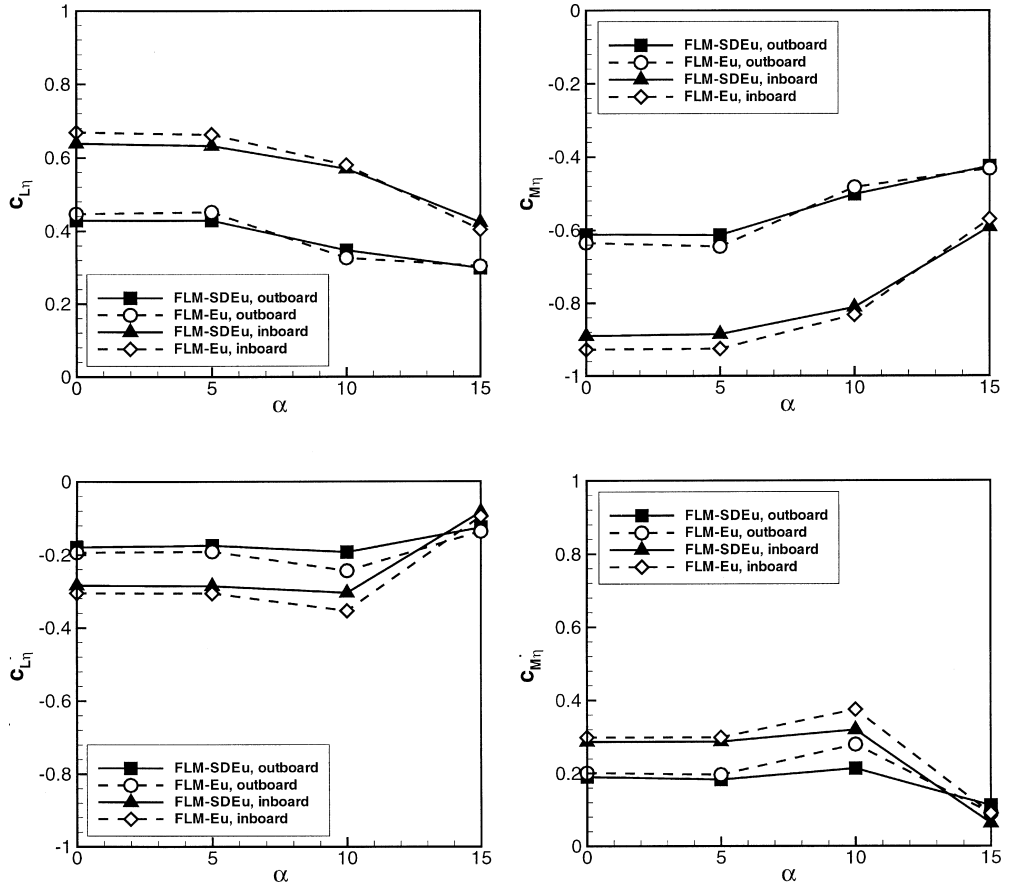

Fig. 8 Stability derivatives of inboard and outboard flap at Mach number $M = 0.8$ and $k = 0.7283$ vs angle of attack.

In the study of the influence of grid resolution, the pressure distribution c_p for the standard grid with 356,400 cells and the fine grid with 652,050 cells is given for the two sections $y/s = 0.35$ and $y/s = 0.75$, when $M = 0.8$ and $\alpha = 0$ deg are chosen (Fig. 5). The pressure distributions with lower pressure on the lower side and higher pressure on the upper side agree with the direction of the tip vortex leading to a negative lift coefficient. The pressure distributions of the standard and the fine grid conform very well, and the lift and pitching moment coefficient show only small deviations with $c_L = -0.05692$ and $c_M = 0.06063$ for the standard grid and $c_L = -0.05711$ and $c_M = 0.06082$ for the fine grid. Further grid convergence studies were not performed because the main objective of this paper is the comparison between the two methods, FLM–SDEu and FLM–Eu, with use of the same grid resolution. Therefore, all of the following simulations are performed with the standard resolution of 356,400 cells.

Pitching Oscillations

The parameters of the investigated pitching oscillations are as follows:

$$\alpha = \alpha_0 + \alpha_1 \sin(k\tau_s)$$

$$\alpha_0 = 0, 5, 10\,\text{deg}, \qquad \alpha_1 = 1\ \text{deg}$$

$$M = 0.8, \qquad x_p = 0.5c_r, \qquad k = 0.5, 2 \tag{2}$$

Figure 6 shows the Lissajous figures for the lift and pitching moment coefficient at the three angles of attack for $k = 0.5$ and 2 and additionally the steady values for α, $\alpha \pm 0.5$, and $\alpha \pm 1$ deg angle of attack. For FLM–SDEu, the values are superimposed from the steady one generated by the nonlinear code FLM–Eu and the first harmonic as the result of FLM–SDEu. For the steady values, the lift and pitching moment coefficient show a linear behavior with the angle of attack for 0 and 5 deg, as expected in this angle of attack region. For 10 deg, c_L and c_M deviate sligthly from linearity with a degressive tendency. The FLM–Eu curves show the cycles with the characteristic start behavior in the beginning. The response is nearly fully developed after the first quarter of oscillation. With increasing reduced frequency, the unsteady values differ more and more from the steady ones. Generally with respect to amplitude and phase, the curves look similar for all α with a shift in the absolute values of c_L and c_M. The conformity between FLM–SDEu and FLM–Eu is very good for all cases, deviations can only be detected at $\alpha = 10$ deg for $k = 0.5$.

Exemplarily, the real and imaginary part of the first harmonic of the pressure distribution c_p at the two sections $y/s = 0.35$ and $y/s = 0.75$ for the two frequencies $k = 0.5$ and $k = 2$ are given in Fig. 7 for $\alpha = 0$ deg and $M = 0.8$. With increasing k, the real part increases. The imaginary part shows characteristics as known for pitching oscillations of an airfoil depending on the rotation point, Mach number, and reduced frequency. In all, the local pressure distributions from FLM–SDEu and FLM–Eu agree very well.

As for the aspect of efficiency of FLM–SDEu, for the pitching oscillations the acceleration lies in the range of 4–12, increasing with decreasing reduced frequency.

Flap Oscillations and Efficiency

Flap efficiency is an important feature of an aircraft and has to be guaranteed over the whole flight envelope. To determine flap efficiency, pitching oscillations of the inboard and the outboard flap are investigated for the freestream Mach number $M = 0.8$ at a wing incidence of 0,5,10, and 15 deg. The harmonic motion of the regarded flap is performed around the flap reference position $\eta_0 = 0$ deg with an amplitude of flap deflection $\eta_1 = 0.4$ deg. The frequency is $f = 6$ Hz, which corresponds to $k = 0.7283$. Flap efficiency is characterized by the stability derivatives $c_{L\eta}$ and $c_{L\dot{\eta}}$ for the lift and $c_{M\eta}$ and $c_{M\dot{\eta}}$ for the pitching moment coefficient. These derivatives can be calculated from the real and imaginary parts of the first harmonic of the coefficients[14]

$$c_{L\eta,M\eta} = \frac{\operatorname{Re} c^1_{L,M}}{\eta_1}, \qquad c_{L\dot{\eta},M\dot{\eta}} = \frac{\operatorname{Im} c^1_{L,M}}{k\eta_1} \tag{3}$$

Figure 8 shows the stability derivatives for the inboard and the outboard flap, respectively, over the angle of attack. The derivatives $c_{L\eta}$ and $c_{M\eta}$ reveal that the inboard flap achieves a higher efficiency than the outboard flap. From the steady flowfield (Fig. 4), it becomes evident that the crossflow velocities in the region of the outboard flap are higher than for the inboard flap, which explains the lower efficiency of the outboard flap. With the increase of angle of attack, the flap effciency is reduced due to the increasing crossflow velocities. When the results of FLM–SDEu are compared with those of FLM–Eu, again the values correspond well.

As an example for a local result, the first harmonic of the pressure distribution is shown in Fig. 9 for the three angles of attack 0, 5, and 10 deg, with regard to the oscillating inboard flap. The chosen section $y/s = 0.35$ cuts the inboard flap area. The real and imaginary part reflect the known characteristics for an oscillating flap in sub- or transonic flow with the singularity at the flap leading edge in the real part and the changing sign in the imaginary part.

The increasing incidence shows only small effects in the curves of the first harmonic, the real part remains nearly unchanged. In the imaginary part, the local values change slightly, but not the general behavior. The deviations between FLM–SDEu and FLM–Eu increase with α, but for interpretation the different scale of the real and imaginary part has to be taken into account.

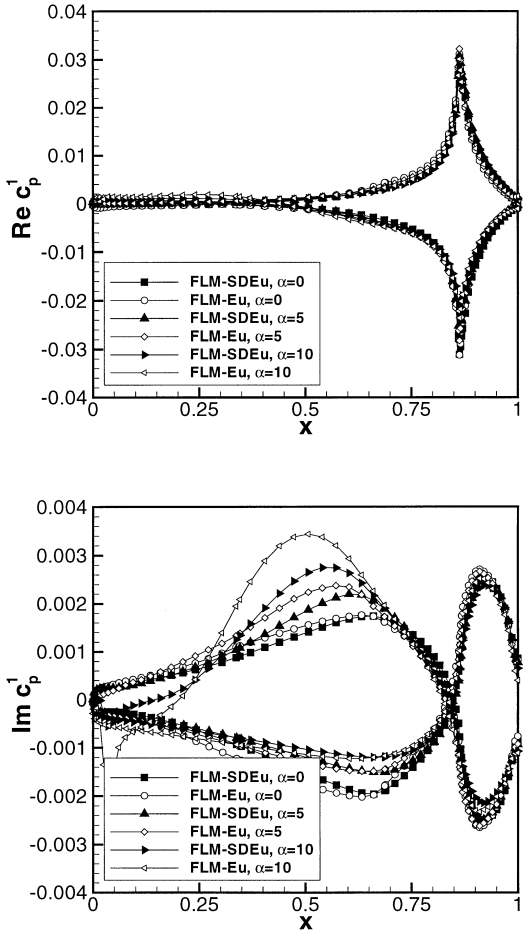

Fig. 9 Real and imaginary part of the first harmonic of the pressure distribution for inboard flap oscillation with $\eta_1 = 0.4$ deg for $\alpha = 0$, 5, and 10 deg at $M = 0.8$ and $k = 0.7283$ in spanwise section $y/s = 0.35$.

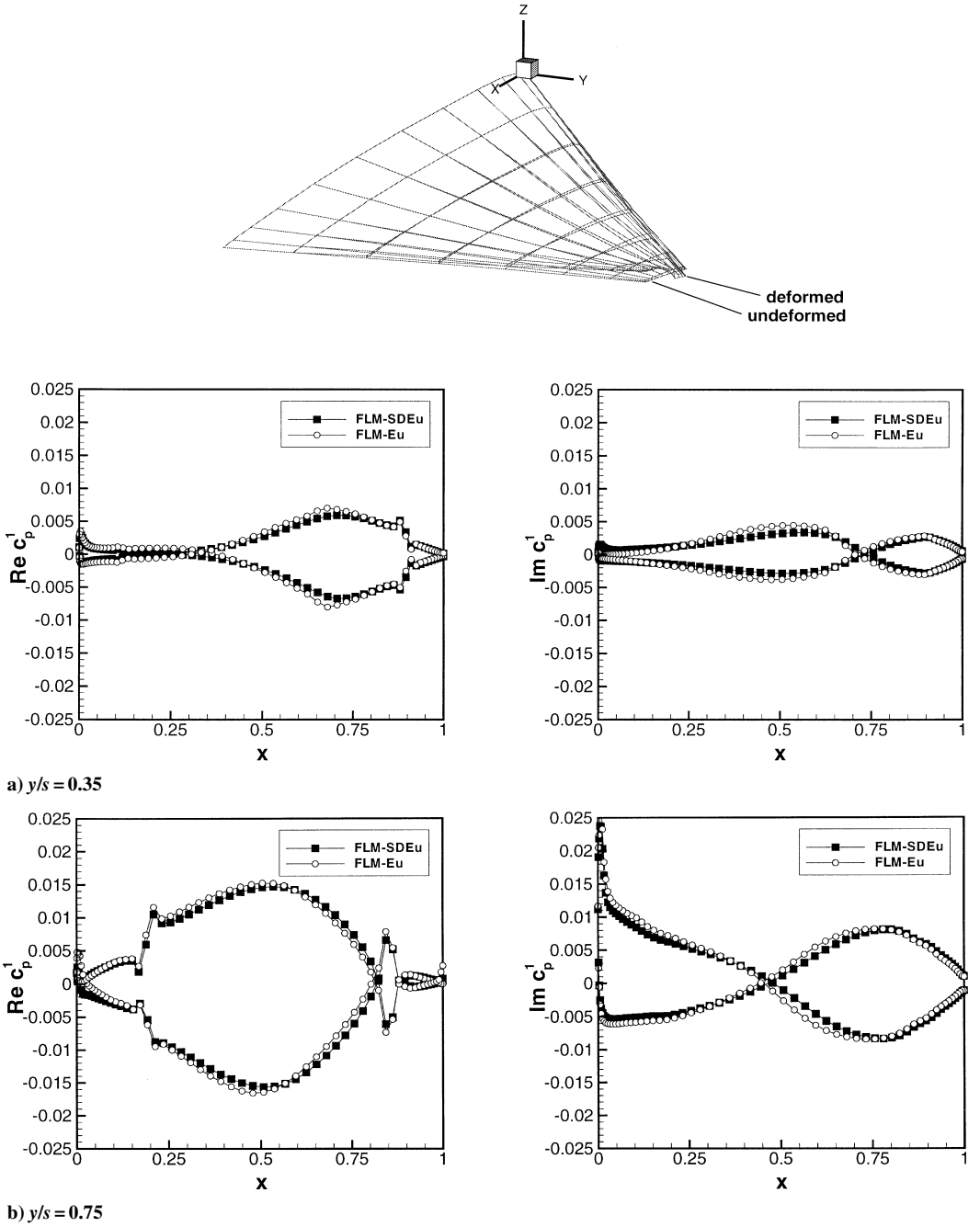

Fig. 10 Real and imaginary part of the first harmonic of the pressure distribution for elastic oscillation for $\alpha = 0$ deg at $M = 0.8$ in spanwise sections $y/s = 0.35$ and $y/s = 0.75$

Elastic Oscillations

For the description of the elastic eigenmodes, an equation with polynomial coefficients for the local amplitudes is used. The regarded elastic eigenform is shown in Fig. 10, the amplitude is superelevated by a factor of 20. The elastic oscillation is performed for $M = 0.8$ at 0-deg angle of attack with a reduced frequency of $k = 1.322$ corresponding to $f = 10.89$ Hz. Figure 10 gives the first harmonic of the pressure distribution for FLM–SDEu and FLM–Eu at the two sections $y/s = 0.35$ and $y/s = 0.75$. The real and imaginary part increase in the spanwise direction due to the increasing deformation. Again, FLM–SDEu and FLM–Eu conform very well. From these simulations, generalized air forces may be calculated, to be used for flutter analysis. More details and further simulations of the elastic eigenmodes may be found in Refs. 15 and 16.

Conclusions

For aeroelastic purposes, where many parameter variations are necessary, methods based on the assumption of small disturbances are attractive due to high-quality results for a reduced CPU time. At FLM–TUM, the method FLM–SDEu was developed to solve the SDEu equations. The method demonstrates the following advantages: applicable to subsonic, transonic, and supersonic Mach numbers with high quality results, reduction of computational time, and compatibility to modal methods.

In this paper, the application of FLM–SDEu on several harmonic motions of a delta wing is presented. The results are compared with the corresponding nonlinear Euler method FLM–Eu, and the flow characteristics are discussed. The overall agreement between both methods is very good. The computational time could be reduced for the cases studied up to now by a factor between 3 and 12 in comparison to the nonlinear code.

Based on FLM–SDEu, the following topics are in work for further refinements: reduction of computing time by implicit time integration, consideration of boundary displacement, inclusion of the second harmonic where necessary, and linearization in the time domain for arbitrary time dependency. Furthermore, a small disturbance

Navier–Stokes method FLM–SDNS is being developed and has already been successfully applied to two-dimensional cases.

Acknowledgments

This work was supported in part by EADS Deutschland GmbH, Military Aircraft Division. The authors thank Jürgen Becker for his kind support and fruitful cooperation over the last years.

References

[1]Silva, W. A., Beran, P. S., Cesnik, C. E. S., Guendel, R. E., Kurdila, A., Prazenica, R. J., Librescu, L., Marzocca, P., and Raveh, D. E., "Reduced-Order Modeling: Cooperative Research and Development at the NASA Langley Research Center," *Proceedings of the International Forum on Aeroelasticity and Structural Dynamics IFASD*, Asociacion de Ingenieros Aeronauticos de Espana, Madrid, 2001, pp. 159–174.

[2]Thomas, J. P., Dowell, E. H., and Hall, K. C., "Three-Dimensional Transonic Aeroelasticity Using Proper Orthogonal Decomposition-Based Reduced-Order Models," *Journal of Aircraft*, Vol. 40, No. 3, 2003, pp. 544–551.

[3]Kreiselmaier, E., "Berechnung instationärer Tragflügelumströmungen auf der Basis der zeitlinearisierten Eulergleichungen," Ph.D. Dissertation, Inst. for Fluid Mechanics, Technische Universität München, Germany, July 1998.

[4]Kreiselmaier, E., and Laschka, B., "Small Disturbance Euler Equations: Efficient and Accurate Tool for Unsteady Load Prediction," 21st Congress of the International Council of the Aeronautical Sciences, ICAS Paper 98-2.6.3, Sept. 1998; also *Journal of Aircraft*, Vol. 37, No. 5, 2000, pp. 770–778.

[5]Hall, K. C., "A Linearized Euler Analysis of Unsteady Flows in Turbomachinery," Ph.D. Dissertation, Dept. of Aeronautics and Astronautics, Massachusetts Inst. of Technology, Cambridge, MA, May 1987.

[6]Hall, K. C., and Crawley, E. F., "Calculation of Unsteady Flows in Turbomachinery Using the Linearized Euler Equations," *AIAA Journal*, Vol. 27, No. 6, 1989, pp. 777–787.

[7]Hall, K. C., and Clark, W. S., "Linearized Euler Predictions of Unsteady Aerodynamic Loads in Cascades," *AIAA Journal*, Vol. 31, No. 3, 1992, pp. 540–550.

[8]Kahl, G., and Klose, A., "Time Linearized Euler Calculations for Unsteady Quasi-3D Cascade Flows," Unsteady Aerodynamics, Aeroacoustics, and Aeroelasticity of Turbomachines and Propellers, edited by H. M. Atassi, Springer-Verlag, New York, 1991, pp. 109–126.

[9]Weishäupl, C., and Laschka, B., "CFD Methods Applied to Non-standard Unsteady Problems in Aircraft-Aerodynamics," *ISASTI 98 Proceedings, 3rd International Symposium on Advanced and Aerospace Science & Technology in Indonesia*, Vol. 1, Indonesian Aeronautics and Astronautics Institute, Jakarta, 1998, pp. 1–14.

[10]Roe, P. L., "Approximate Riemann Solvers, Parameter Vectors and Difference Schemes," *Journal of Computational Physics*, Vol. 43, No. 2, 1981, pp. 357–372.

[11]Jameson, A., and Turkel, E., "Implicit Schemes and LU-Decompositions," *Mathematics of Computation*, Vol. 37, No. 156, 1981, pp. 385–397.

[12]Weishäupl, C., and Laschka, B., "Nonlinear and Small-Disturbance Euler (SDEu) Calculations for Delta Wing Flap Efficiency," AIAA Paper 2000-0124, Jan. 2000.

[13]Weishäupl, C., and Laschka, B., "Calculation of Unsteady Aerodynamic Forces using the Small Disturbance Euler Equations (SDEu)," *Proceedings of the International Forum on Aeroelasticity and Structural Dynamics IFASD*, Asociacion de Ingenieros Aeronauticos de Espana, Madrid, 2001, pp. 211–224.

[14]Weishäupl, C., Pechloff, A., and Sickmüller, U., "Instationäre Luftkräfte bei Klappenschwingungen mit Hilfe der Euler Gleichungen für kleine Störungen (SDEu)," Inst. for Fluid Mechanics, Rept. TUM-FLM-99/26, Technische Universität München, Germany, Dec. 1999.

[15]Sickmüller, U., Weishäupl, C., and Pechloff, A., "Instationäre Luftkräfte bei verschiedenen Eigenformen mit Hilfe der Euler Gleichungen für kleine Störungen (SDEu)," Inst. for Fluid Mechanics, Rept. TUM-FLM-2001/02, Technische Universität München, Germany, Jan. 2001.

[16]Sickmüller, U., Pechloff, A., Weishäupl, C., and Laschka, B., "Aerodynamische Untersuchungen eines Deltaflügels bei verschiedenen Eigenformen mittels eines Euler-Verfahrens bei kleinen Störungen," Deutscher Luft- und Raumfahrtkongress 2001, Rept. DGLR-2001-065, Hamburg, Germany, 17–20, Sept. 2001.

[17]Brodersen, O., Ronzheimer, A., Hepperle, M., Schenk, M., and Wild, J., "Einführung in die Bedienung und Weiterentwicklung des Programmsystems MEGACADS," Technical Report, Inst. für Entwurfsaerodynamik, DLR, German Aerospace Research Center, Braunschweig, March 1996.